

ACCURACY OF CFD CODES IN THE PREDICTION OF PLANING SURFACES HYDRODYAMIC CHARACTERISTICS

Stefano Brizzolara, Francesco Serra

University of Genoa, Department of Naval Architecture and Marine Technology, Italy

SUMMARY

The application of CFD methods for fast planing hulls is at present a reality not only at research level but also by designers and hydrodynamic consultants in the design studies of fast planing yachts and racing boats. But have these tools been accurately tested in these type of free surface flows? Is their level of accuracy known at least on simple planing hull shapes? The present paper intends to address, at least from a preliminary point of view, some of these crucial question that should interest naval architects, designers and hydrodynamic researchers who share this field of interest. For this purpose an extensive study using an up to date RANSE VOF solver with free surface tracking capability, has been performed, testing the method on a wedge shaped prismatic planing hull, having a constant deadrise angle of 20 degrees, systematically varying the running trim angle and wetted length.

Results obtained, in terms of drag lift forces and longitudinal trimming moment, are compared with available experimental (model tests made at Hydronautics towing tank) and semi-empirical theories (Savitsky, Shuford, etc.) commonly used by naval architect for the prediction of planing surface hydrodynamic performance.

By the comparison of global force components and moments and the analysis of distributed parameters, such as pressure on the wetted hull, tangential stresses, spray root line and wave elevations, some interesting conclusions can be drawn on the accuracy of CFD codes for the prediction of steady hydrodynamic performance of planing hulls.

1. INTRODUCTION

It is at present not rare to get into the proposal for the application of RANSE codes for the prediction of the hydrodynamic characteristics of fast planing boat hulls. Different designers and shipyards, in this field, are in these days looking to CFD studies to even substitute towing tank tests in the design studies of their hulls. But while for conventional displacement ships there is a wide literature and several international CFD workshops dedicated to the correlation of different RANSE method results to experimental measurements, for fast planing hulls there is much less information.

In general, the peculiar difficulty that characterises the resistance prediction of planing hulls is that both its viscous and pressure components are related in a non-linear way to the dynamic lift force and trim moment developed by the complex flow on the hull at high speeds. Indeed in these cases, the accurate prediction of running trim and sinkage, and hence the lift force component and its longitudinal moment is of fundamental importance.

Historically, as well known, the hydrodynamic characteristics of planing surfaces were first studied through experiments on a large systematic series of tests made between 1940 and 1960 at the towing tank of NACA in Langley and at Davidson laboratory. On the basis of these tests, some attempts for the interpretation of the results have been made and several relations were developed for the estimation of hydrodynamic forces acting on planing surfaces of simple geometrical shapes.

It is somehow remarkable that some of these semi-empirical methods are still nowadays widely employed for the design of fast planing hulls, constituting the practical "state of the art" in the field. The most widely dif-

fused being the method proposed by Savitsky (1964) which account for the old mentioned experimental results to solve the more general hydrodynamic problem of a fast hull running in steady condition (dynamic equilibrium) in a pure planing regime.

From a pure hydrodynamic point of view, the typical flow pattern around planing hulls of general shapes is rather complex and not easy to be accurately solved from a theoretical point of view.

In fact, some attempts of developing theoretical / numerical methods that could cope with this complex flow physics have appeared only in recent years, the most recent one being that proposed by Savander (2002) which among the other is the only able to accurately allow for the solution of the spray root. These methods, though, are still based on several fundamental simplification, as they reduce the 3D problem to the solution of a series of 2D potential flow problems on the hull transverse sections. In any case, these methods are able to overcome the inherent limitation of Savitsky method, rigorously valid only for prismatic hull shapes, extending the possibility to estimate the hydrodynamic characteristics of hulls with warped sections and cambered chine and keel lines. A review of different 2D theoretical models, based on potential flow theory, with a preliminary comparison of the results obtained in one case also against RANSE method, is presented by Pemberton et al. (2001).

In this panorama, the present systematic study is positioned, aiming to the assessment of the applicability of RANSE methods for the evaluation of dynamic forces and moment acting on simple constant deadrise prismatic planing surfaces. The study has been carried out at the University of Genoa as a preliminary investigation in

the framework of a more general research project with a large Italian pleasure yacht building group.

To the authors' knowledge very few other examples of similar systematic studies about CFD methods have been released in the open literature: a recent example is that of Caponnetto (2001), who limited his comparison to the pressure force and moment predicted with RANSE solver on prismatic hull forms versus Savitsky's formulae. His study confirms the general conclusions about the order of magnitude of CFD computation accuracy, obtained in the present study, but the comparison of the CFD results only against Savitsky theory, which is already an interpretation of physical data and can be affected by a certain inherent approximation, somehow limits the generality of his conclusions.

The CFD results obtained in the present study, on the contrary, have been programmed on the basis of the available experimental tests cases and compared in the paper with experimental measurements and interpretation theories. The next section introduces the reference experimental data and trying to provide also an analysis on the indirect and direct errors that affect the measurements of trimming moment and force components.

2. THE EXPERIMENTAL REFERENCE TESTS

The CFD calculation cases have been selected from the well known series of tests done by Chambliss and Boyd (1953) in the fast towing tank of Langley. The tests regarded two different prismatic planing surfaces with deadrise of 20 deg and 40 deg kept constant along the length. An overview of the model with 20 deg deadrise, used in those tests and assumed as the reference model for the CFD studies is given in figure 1. Its main dimensions are 1 meter in length, 10cm in maximum breadth at chines.

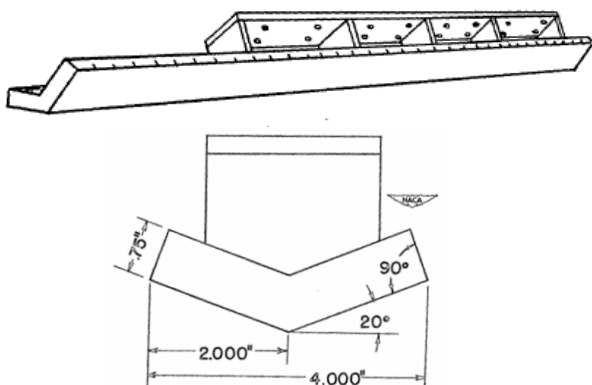


Figure 1

The 20 deg deadrise prismatic model tested by Chambliss and Boyd (1953)

The towing carriage used for these tests was conceived, as per figure 2, in such a way to keep the given trim and load (weight) of the model during towing, while leaving it free to surge at high speed. In this way, the model balanced in static condition, was let free to vary its draft at

different towing speed, assuming the its final dynamic draft and wetted length. During the tests, the drag R (horizontal force component) and the draft were measured, the lift force L (vertical component) was not measured and by assumption taken as equal to the displacement of the hull at rest. The wetted length at chine L_c and at keel L_k was recorded by visual observation from the tank bottom.

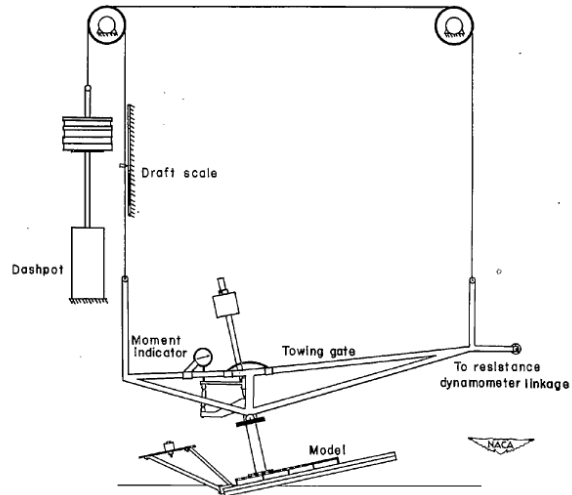


Figure 2

The towing carriage used by Chambliss and Boyd

An extract of the test matrix showing the initially cases selected for CFD calculations is given in Table 1: all the cases refer to the prismatic model having 20 deg of deadrise. Three cases for each of the different trim angles (2, 4 and 6 degrees) were selected to cover a wide range of variation of the other parameters: Froude number and load (lift) coefficient. Four additional cases successively simulated for detailing the validation of the cases with of results. The table reports also the value of the non-dimensional load coefficient C_Δ , (equal to the lift coefficient by assumption), the resistance coefficient C_R , the corresponding Froude number C_v , the wetted lengths and the longitudinal position of the centre of pressure, calculated from the measured trimming moment, according the formula given in the list of symbols, in the last section.

Table 1

Selected cases from the exp. tests of Chambliss and Boyd

Case #	Trim τ	$C_{L \text{ EXP}}$	$C_{R \text{ EXP}}$	C_v	$(L_c / b) \text{ EXP}$	$(L_m / b) \text{ EXP}$	$(L_k / b) \text{ EXP}$	$(L_p / b) \text{ EXP}$
Prova1	2°	4,26	2,06	19,89	0,68	2,19	3,70	1,59
Prova2	2°	4,26	5,56	13,48	5,50	6,97	8,42	4,86
Prova3	2°	6,39	3,39	17,02	5,00	6,50	8,00	3,90
Prova4	4°	0,85	0,12	6,16	0,38	1,09	1,80	0,63
Prova5	4°	6,39	1,69	10,28	5,88	6,59	7,30	4,59
Prova6	4°	10,65	2,81	16,16	3,00	3,72	4,42	2,85
Prova7	6°	0,85	0,14	4,67	0,50	1,00	1,50	0,63
Prova8	6°	6,39	1,34	10,34	2,25	3,25	3,25	2,04
Prova9	6°	10,65	2,38	11,04	4,50	5,00	5,50	3,27

It is sensible to argue about the order of magnitude of the direct and indirect errors that affect the measured or experimentally derived hydrodynamic characteristics. The absolute error related to the accuracy of the measuring equipment, as indicated in the original NACA report,

generate relative errors which, for the selected test cases, have the following mean and maximum values :

- on lift ϵ_{Δ} = mean 3%, max 8% ;
- on resistance ϵ_R = mean 20% max 50% ;
- on velocity ϵ_V = mean 0.7% max 1.3% ;
- on draft ϵ_D = mean 5% max 10% ;
- on keel wetted length ϵ_{Lk} = mean 1% max 3% ;
- on trim angle ϵ_{τ} = mean 2% max 5% ;

The order of magnitude of the above indicated relative errors accounts for the direct measurement accuracy only, not including any other indirect error caused by a defect of accuracy on These order of accuracy on tests results is confirmed also by Payne (1995) who collated the results of various experiments of that time, to develop his theory. To have an idea of the repeatability of the measurements, in Table 2, the results obtained in two repeated tests have been extracted and highlighted from the original report of Chambliss and Boyd (1953).

It is worth to note at this point that all the semi-empirical formulations successively developed (for instance those by Savitsky or Shuford) have tried to interpret these tests results and in fact in many cases show a large deviation from them, as demonstrated in the section dedicated to the analysis of results. When validating the results obtained with a certain theoretical/numerical mode against these experimental tests, one should bear in mind the order of accuracy above mentioned.

Table 2

Extract of test runs to show the measurement scattering (from Chambliss and Boyd, 1953)

Trim, τ , deg	C_D	C_T	C_R	$\frac{l_a}{b}$	$\frac{l_b}{b}$	$\frac{l_k}{b}$	$\frac{l_p}{b}$	C_{Lb}	C_{Db}
2	0.85	9.27	0.37	0	1.47	2.92	2.49	0.0198	0.0073
2	2.13	9.67	1.01	3.75	5.22	6.68	3.42	.0456	.0216
2	2.13	7.70	.90	3.08	4.52	5.95	2.94	.0453	.0191
2	2.13	14.64	.93	0	1.47	2.92	1.80	.0200	.0087
2	4.26	13.48	5.56	5.50	6.97	8.42	4.06	.0468	.0262
2	4.26	13.54	2.17	4.50	5.97	7.42	3.39	.0455	.0236
2	4.26	19.89	2.06	.68	2.19	3.70	1.59	.0216	.0104
2	4.26	20.65	1.98	.62	2.09	3.55	1.59	.0200	.0093
2	4.26	23.12	2.04	0	1.47	2.92	1.50	.0158	.0076
2	6.39	16.78	3.62	---	---	---	4.59	.0455	.0258
2	6.39	17.02	3.32	4.25	5.72	7.18	4.05	.0441	.0229
2	6.39	17.02	3.39	5.00	6.50	8.00	3.90	.0441	.0213
2	6.39	20.04	2.84	1.88	3.34	4.80	2.52	.0318	.0141
2	6.39	20.04	3.04	3.95	3.47	5.00	2.13	.0318	.0151
2	6.39	25.50	2.55	0	1.47	2.92	1.26	.0196	.0078
4	.85	6.16	.12	.38	1.09	1.80	.63	.0448	.0063
4	2.13	7.32	.49	2.80	3.52	4.22	2.43	.0792	.0184
4	2.13	7.38	.46	2.22	2.96	3.70	1.67	.0782	.0169
4	6.39	10.16	1.67	5.88	6.59	7.30	4.38	.1235	.0323
4	6.39	10.28	1.69	5.88	6.59	7.30	4.59	.1209	.0320
4	6.39	12.77	1.96	2.90	3.22	3.92	2.28	.0785	.0192
4	6.39	12.81	1.64	2.75	3.46	4.18	2.52	.0772	.0200

3. THE CFD MODELS

The RANSE code Star-CD has been used for preparing solving and analysing the cases presented. The solver is an up to date volume of fluid RANSE solver, able to deal with standard regular (hexahedral, tetrahedral, prismatic, etc.) or more unusual irregular (polyhedral, trimmed cells) mesh cells. For what concerns this application, the solver has the capability to consider a wide spectrum of turbulence models, including the high Reynolds number k-ε model, adopted for the calculations and a two layers wall function extrapolation. For flows with sharp air/water interface the solver uses a proprietary type of free surface capturing method based on the volume of fluid (VOF) method, i.e. on the solution of a set of non-

linear equation that regulate the advection and dispersion of this new scalar variable in the whole flow domain. In the regions with mixed fluid (0<VOF<1) the standard RANS and continuity equations are solved as for a single fluid, but the density and kinematic viscosity of this mixed fluid are assumed to be expressed as a weighted average of the two fluid densities and kinematic viscosity, averaged with the volume fraction of each fluid present in the cell. The method for solving the free surface flow is rather efficient in the framework of finite volumes RANSE methods and, as demonstrated later, can lead to a very effective description of complicated flows such as that in the spray region of planing hulls.

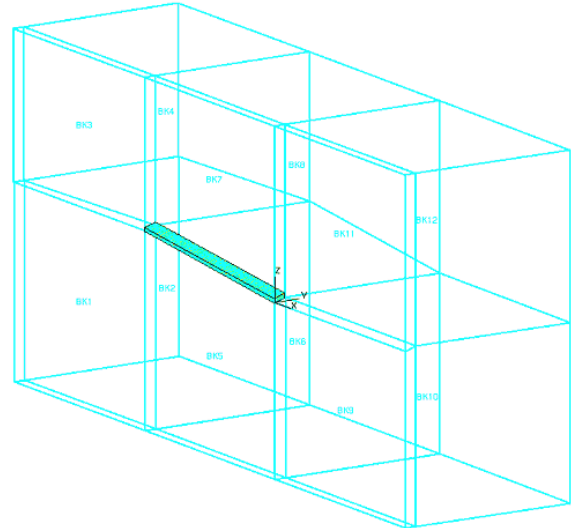


Figure 3

Volume Mesh Decomposition in 12 sub-volume plus the front bock

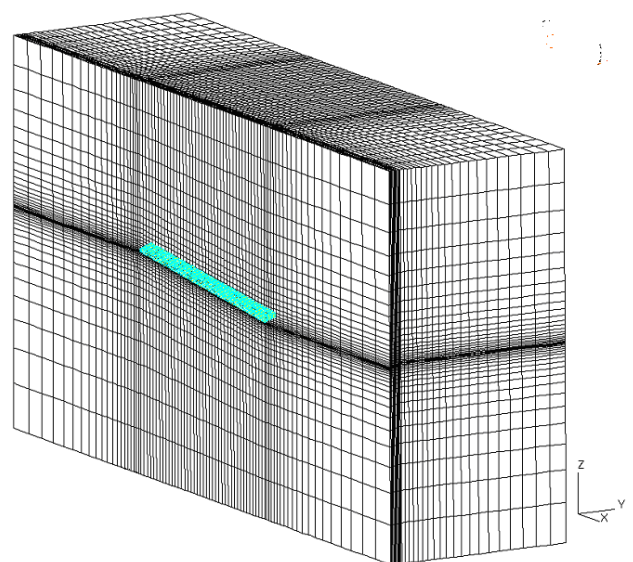


Figure 4

Volume Mesh (half volume depicted, for symmetry)

A structured type volume mesh has been created for all the simulated cases by an automatic script written for the purpose on the basis of the inline functions of the Pro-AM pre-processor. The volume mesh is divided in 12

sub-regions, as depicted in figure 3. Each block is decomposed in prismatic cells parametrically refined close to the wedge bottom. The script was written in order to generate automatically the volume mesh, given the trim angle of the prismatic surface and the running draft. An example of this result is represented in figure 4, with the close up view on a transversal section of figure 5.

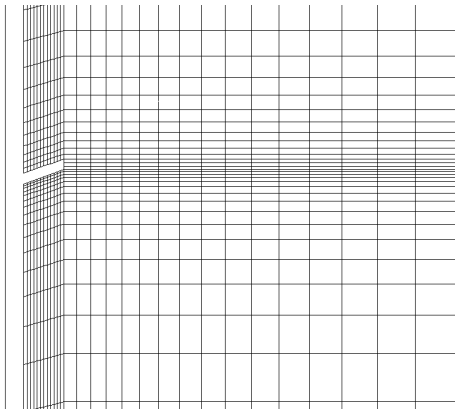


Figure 5

Detail of grid refinement close to the wedge (transverse section)

Three further refinements have been applied to the initial mesh: the first refinement interests a volume in a conical region behind the estimated stagnation point on the keel line, so to accurately resolve the wave formation in the planing hull wake (figure 6); the second refinement has been applied to the three layers of cells close to the hull bottom surface, by subdividing each cell dimension in the layer by a factor two; the third refinement interests only the closest layer to the planing surface and has been applied to obtain a correct value of the $y^+ = \rho \cdot C_\mu^{1/4} \cdot k^{1/2} \cdot y / \mu$ (in which C_μ is the coefficient of turbulent viscosity, k is the Von Karman constant and μ the molecular viscosity of the water) of the first layer of cells close to the wall, in order to guarantee a correct resolution of the boundary layer region.

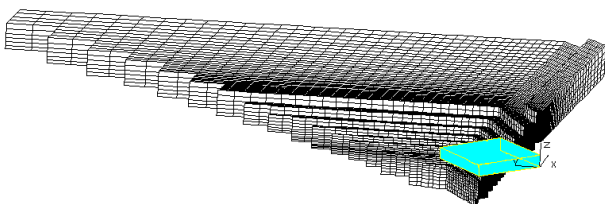


Figure 6

First refinement done in a conical region behind the stagnation point on the keel line

A preliminary sensitivity analysis has brought to the selection of the minimum number of cells to ensure the convergence of the CFD results in terms of global hydrodynamic forces. Eventually, a total number of about 250'00 volume cells has been used for each of the simulated cases. All the simulated cases, then, had absolutely similar mesh typology and relative refinement ratios.

Boundary conditions used are: inlet with prescribed uniform velocity, constant depth flow, non-slip on the planing surface, slip on the bottom and on the lateral boundary of the domain, constant piezometric pressure for the outlet (to avoid reflections of the wave formation and to introduce the least conditioning to the forward flow), obviously on the internal domain surface a symmetry plane condition.

The selected turbulence model is the linear $k-\epsilon$ model for high Reynolds numbers, with standard algebraic wall functions. The parameters of the turbulence model at inlet were set as $k=0.0013 \text{ m}^2/\text{s}^2$; $\epsilon=0.00109 \text{ m}^2/\text{s}^3$ after checking, in a series of preliminary calculations, the value of turbulence viscosity and viscosity ratio close to the planing surface.

4. ANALYSIS OF THE RESULTS

In order to compare CFD results directly with the mentioned model tests, all the calculations were performed in model scale. The model was fixed at the trim angle and draft at keel (where the pile up is negligible) of the nine experimental reference cases. For each of these cases, table 3 presents the advance speed, trim angles and corresponding draft of the keel at transom. As noted, for each running trim the draft conditions were chosen in order to explore a wider range of planing flow regimes, corresponding almost to a condition of no chine wet and medium/long wetted chine length.

The free surface solution, evolving from the initial undisturbed condition, requires to use the unsteady solver and to stop when a satisfactory convergence of the dynamic forces and moments is achieved. The convergence is achieved almost immediately, after few hundreds of seconds. The simulations used an initial time step of 10^{-5} s from $t=0$ s to $t=0.001$ s, then the time step was increased to 10^{-4} s until a total time of about $0.5 \div 0.8$ s depending on the advance speed.

The comparison with

4.1. COMPARISON WITH MODEL TESTS RESULTS

As already mentioned, being the simulations done with the model fixed in the experimental attitude, the validation has to include not only the resistance but also the lift component.

The comparison between the numerical and experimental results is presented in the graphs and tables of figure 7 and 8, for the total lift and drag components respectively. The values of the forces are total values, as they are calculated from the CFD normal and tangential stresses. In this way they are readily comparable with the model test measurements, including the viscous and pressure (dynamic and static) components. When more than one run was for the same running condition was available from model test database, the relative experimental values have been calculated by a reasoned average, excluding

C_L	EXP	NUM	% Diff
case 1	4.26	4.69	10%
case 2	4.26	4.22	-1%
case 3	6.39	5.99	-6%
case 4	0.85	0.75	-12%
case 5	6.39	6.30	-1%
case 6	10.65	9.98	-6%
case 7	0.85	0.87	2%
case 8	6.39	6.34	-1%
case 9	10.65	10.22	-4%

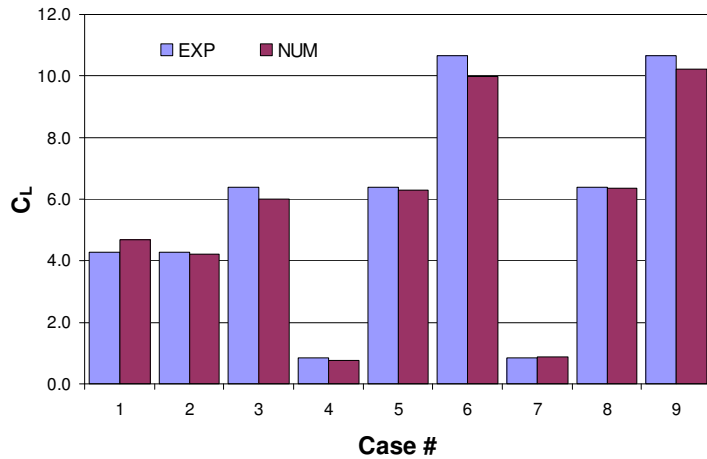


Figure 7

Comparison of CFD prediction of total (viscous+pressure) Lift with corresponding experimental values

C_R	EXP	NUM	% Diff
case 1	2.00	1.57	-21%
case 2	2.17	1.98	-9%
case 3	3.36	3.03	-10%
case 4	0.14	0.125	-11%
case 5	1.69	1.66	-2%
case 6	2.74	2.24	-18%
case 7	0.14	0.131	-6%
case 8	1.30	1.21	-7%
case 9	2.33	2.16	-7%

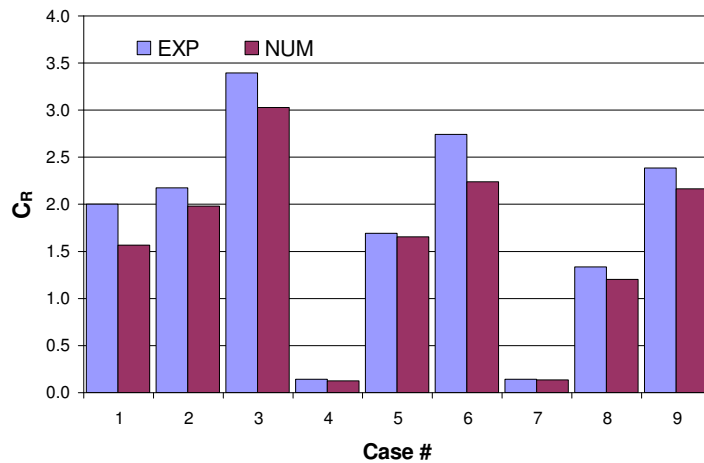


Figure 8

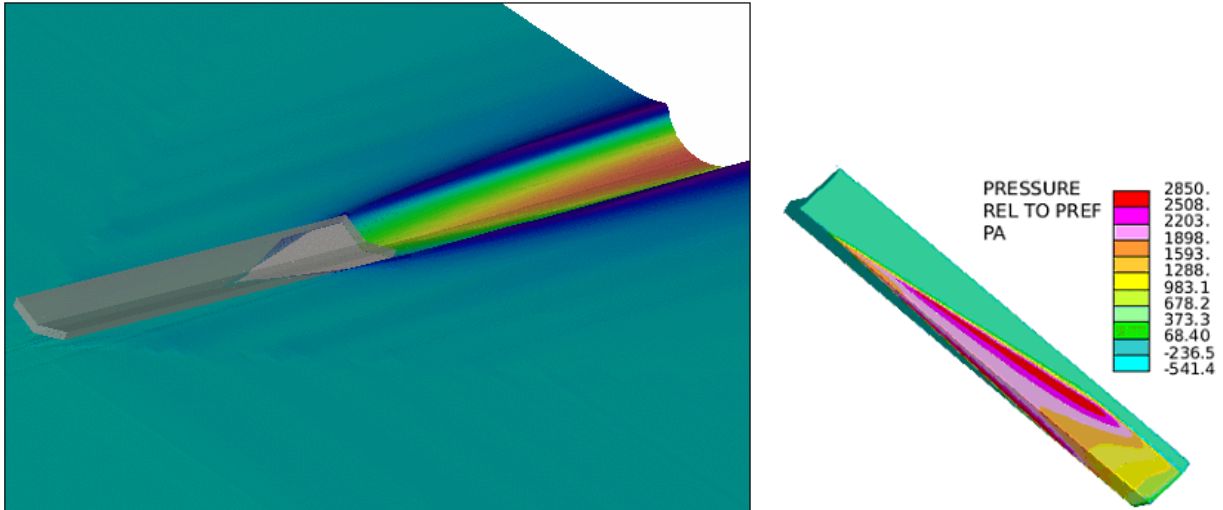
Comparison of CFD prediction of total (viscous+pressure) Drag with corresponding experimental values

Table 3

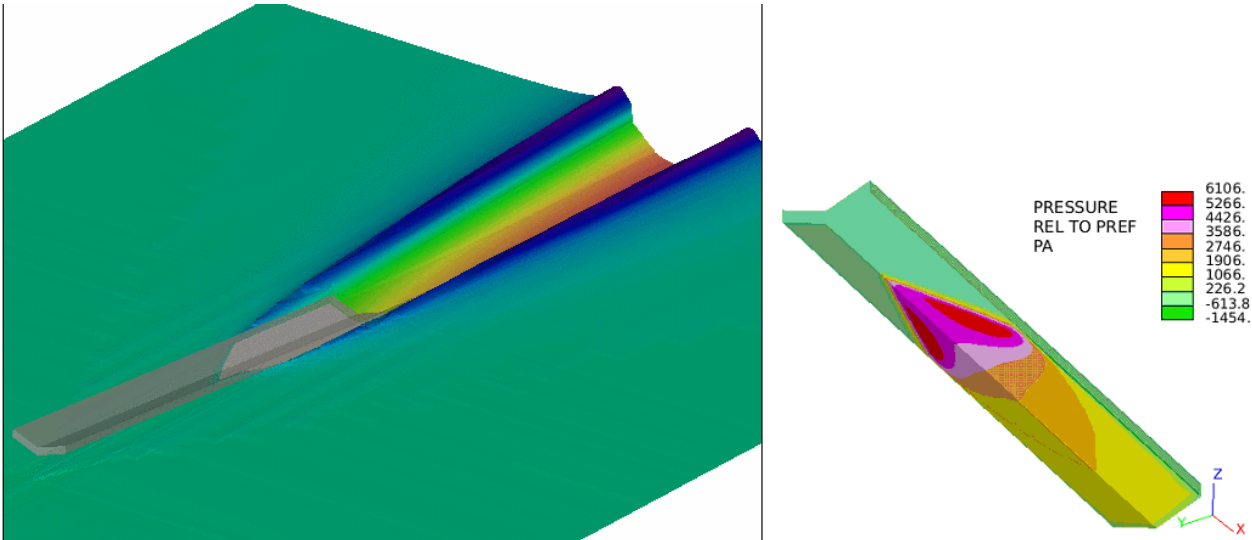
Draft and speed conditions for the nine reference cases;
Comparison of CFD and experimental wetted lengths (both taken by visual observation)

Case #	prova1	prova2	prova3	prova4	prova5	prova6	prova7	prova8	prova9
<i>Experimental Results:</i>									
trim	2	2	2	4	4	4	6	6	6
Cv	19.89	13.48	17.02	6.16	10.28	16.16	4.67	10.34	11.04
Vel. [m/s]	19.86	13.46	16.99	6.15	10.26	16.13	4.66	10.32	11.02
Draft [m]	0.01372	0.02997	0.02946	0.0128	0.05171	0.0315	0.01595	0.0345	0.0579
L_k/b_{exp}	3.7	8.42	8	1.8	7.3	4.42	1.5	3.25	5.5
L_k/b_{exp} [m]	0.376	0.855	0.813	0.183	0.742	0.449	0.152	0.330	0.559
L_c/b_{exp}	0.68	5.5	5	0.38	5.88	3	0.5	2.25	4.5
L_c/b_{exp} [m]	0.069	0.559	0.508	0.039	0.597	0.305	0.051	0.229	0.457
L_m/b_{exp}	2.19	6.97	6.5	1.09	6.59	3.72	1	2.75	5
L_m/b_{exp} [m]	0.223	0.708	0.660	0.111	0.670	0.378	0.102	0.279	0.508
<i>Numerical Results:</i>									
L_k_{num} [m]	0.38	0.87	0.83	0.19	0.75	0.46	0.16	0.34	0.56
L_c_{num} [m]	0.085	0.58	0.53	0.042	0.61	0.322	0.065	0.25	0.475
L_m_{num} [m]	0.2325	0.725	0.68	0.116	0.68	0.391	0.1125	0.295	0.520
λ_{num}	2.29	7.14	6.69	1.14	6.69	3.85	1.11	2.90	5.11
<i>Relative Differences:</i>									
Diff. % $L_k_{num-exp}$	1.1%	1.7%	2.1%	3.9%	1.1%	2.4%	5.0%	3.0%	0.9%
Diff. % $L_c_{num-exp}$	23.0%	3.8%	4.3%	8.8%	2.1%	5.6%	28.0%	9.4%	3.9%
Diff. % $L_m_{num-exp}$	4.5%	2.4%	3.0%	4.7%	1.6%	3.5%	10.7%	5.6%	2.3%

CASE 1 - Trim=2°; V=19.86m/s ; Draft=1.37cm



CASE 6 - Trim=4°; V=16.3m/s ; Draft=2.15cm



CASE 7 - Trim=6°; V=4.66m/s ; Draft=1.60cm

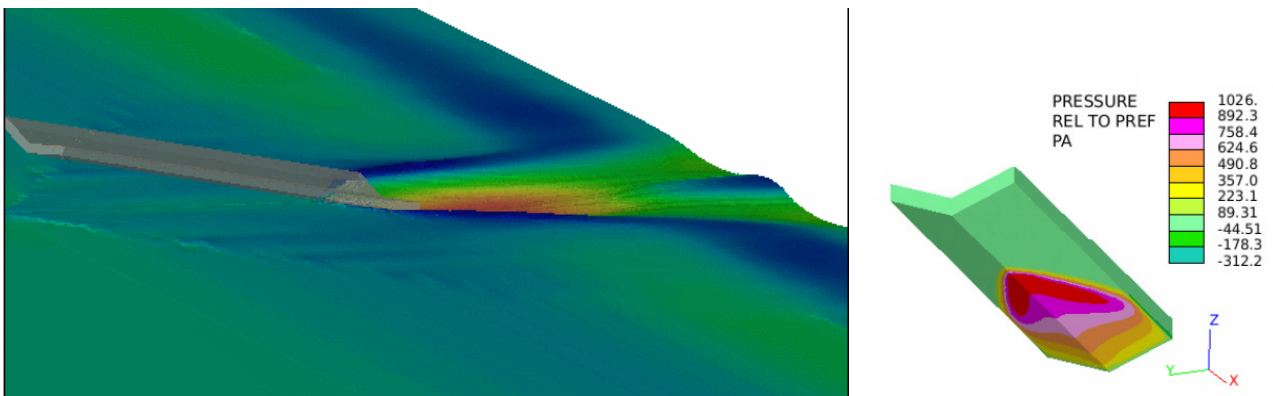


Figure 9
Comparison of CFD (viscous) Drag and measured experimental value

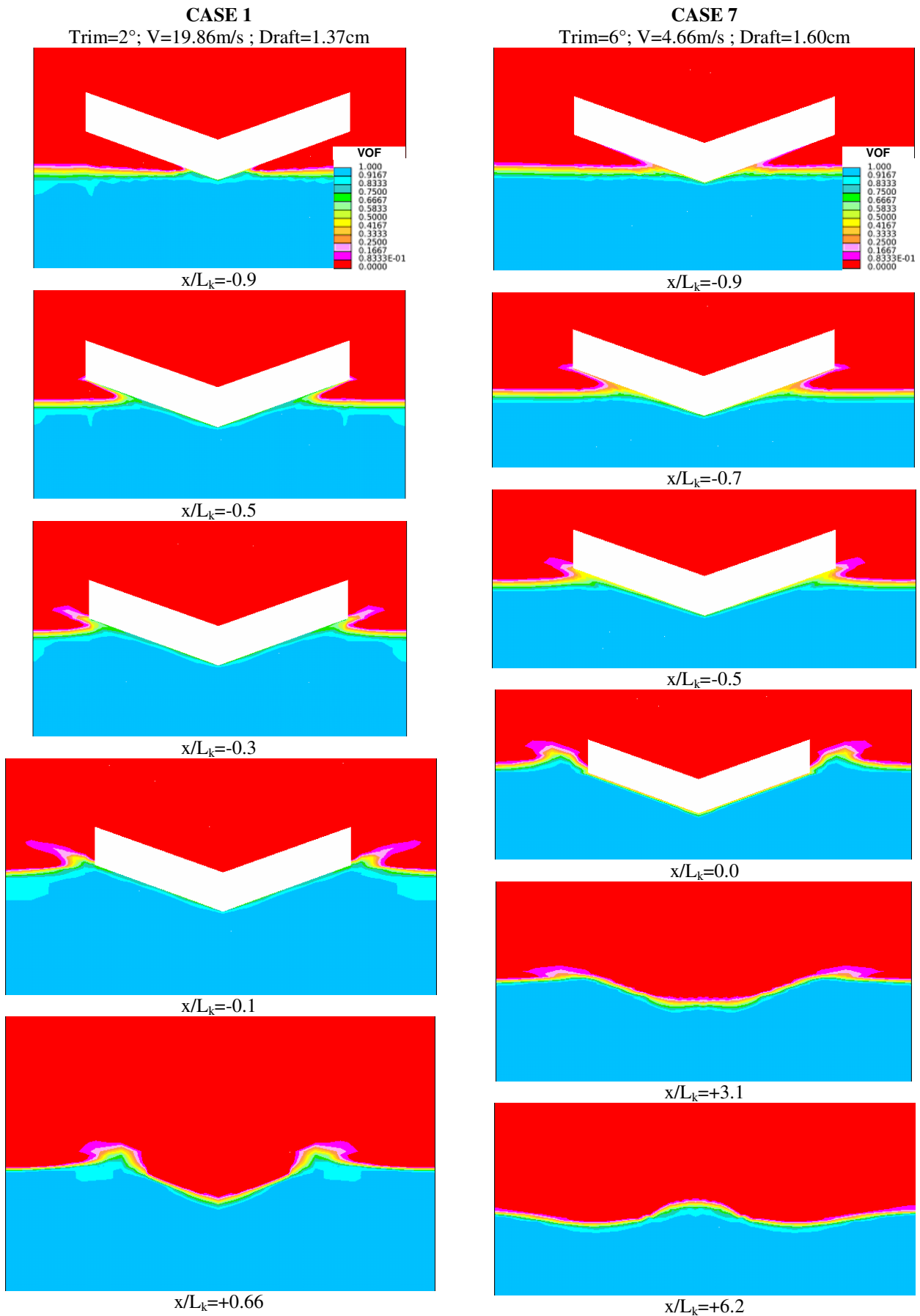


Figure 10

VOF distribution predicted for two different cases. Free surface is assumed to correspond to VOF=0.5 (yellow)

non-realistic measurements. For instance, two runs having the same load coefficient and almost the same speed are available for case 2 (highlighted in yellow in table 2), but among only the results of the second run with $C_R=2.17$ were taken as valid for comparison, since the first run is evidently too out of scale.

Overall, the correlation of the obtained numerical results with the experiments appears sufficiently good, being the numerical relative divergence generally contained inside the relative accuracy of the measuring equipment already highlighted in the section 2 of the paper. In fact the mean deviation in lift is around 5%, while the deviation is in the average around 12%.

The general trend of the RANSE to underestimate the lift and consequently the drag is noted: in fact, where the numerical lift deficiency is higher also the drag is (cases 4, 3 and 6). Case 1 seems to follow a story apart, the numerical lift resulting is higher than the experimental, while drag much lower. This case results to have a very high speed, and perhaps other physical phenomena, such as wind force and spray disturbance can affect the results. Wind resistance was neglected in the calculation of the forces with RANSE, while in the experiment it is expected that some effect of the air flow should be present, though the carriage was in some way protected with wind shield.

Interesting is also the quantitative comparison of the predicted wetted portion of the hull, as presented in table 3. Since the draft of the model was set to correspond to the wetted keel length measured during the run (neglecting the pile up of the flow at keel), there is no surprise to see its good correlation. Different is instead the wetted length at chines, which depend from the correct prediction of the spray root region. In the average, a good correlation is noted also on as regards this parameter, except for case 1 and case 7, where it is believed that the small value of the absolute wetted length may suffer from the higher measuring relative inaccuracy. Incidentally, it is worth noting that also the numerical wetted lengths are evaluated by visual observation and not directly calculated, so also they can be result affected by a measurement error.

The wetted area of the hull is visible also from the graphs on the left side of figure 10. These graphs show the free surface height calculated in the near field by RANSE code. The hull surface was drawn as a transparent object, so its part on the bottom that is touched by water (wetted portion) appears in a clearer grey colour. The separation line between the two grey areas is in fact the spray root line. The intersection of this spray root line with the keel and the chines was used to evaluate their respective wetted lengths.

The free surface deformation is very well rendered by the contour plots of the VF variable on transversal sections at different longitudinal locations along the planing surface and in the wake. Figure 10 presents case-1 with 2° trim and case-7 with 6° trim angle, the same already analysed in figure 9. The drawn contours represent the value of the volume fraction (VF) which express the concentration of water with respect to air into a calculation cell. This pa-

rameter is solved in each cell and can continuously vary between 0 (air) and 1 (water). Conventionally the free surface is thought as coincident with the contour surface having $VF=0.5$ (yellow contour in the plots of figure 10). So cells having a $VF<0.5$ can be thought as interested by a flow mixture of air and water, a kind of spray. The jet spray once detached from the chine is bent down to the free surface by the gravity force and is re-dispersed there. The wavy wake aft of the transom stern seems also well captured and in accordance with what experimentally measured by Korvin-Kroukovsky, Savitsky et al. (1948). The proper qualitative resolution of the free surface deformation in the spray root region and the correct capturing of the flow in the jet spray region, in addition to the quantitative verification of the hull wetted lengths, seem to confirm that the RANSE solver is able to correctly consider all the main physical phenomena involved in the planing regime. The same cannot be said for the other theoretical method mentioned in the introduction, which necessarily make a series of simplifications.

4.2 COMPARISON WITH SEMI-EMPIRICAL FORMULATIONS

After the initial validation phase against experimental results, a second verification has been done of the numerical calculations against known semi-empirical formulations. Among many existing, the two of Savitsky (1964) and Shuford (1956), developed and so strictly valid for prismatic bodies were selected. It is beyond the scope of the paper to illustrate the semi-empirical formulations achieved by these two scientists.

Four additional simulation cases, whose main particulars are given in Table 4, have been added to those already described in Table 3, with the intention to achieve a higher resolution in the numerical description of the dependence of drag lift and trim moment on the mean wetted length.

Table 4
Additional Simulation Cases

Case	Trim (deg)	C_Δ	C_R	C_V	Vel. (m/s)	λ_{exp}
prova10	4°	10.65	2.50	18.45	18.42	2.21
prova11	4°	6.39	1.45	20.07	20.04	0.71
prova12	4°	19.17	5.13	19.83	19.80	5.25
prova13	4°	19.17	5.30	17.35	17.32	7.41

The comparison between numerical calculations and these two usual formulations offers the chance to validate also these two semi-empirical theories with the experimental results. For this purpose all the correlation graphs of figure 11 12 and 13 include not only the Savitsky and Shuford results, but also the values derived from the complete test series of Chambliss and Boyd (1953).

The comparison of predicted lift values with the experimental data is presented in the three plots of figure 11, for trim angles of 2, 4, 5 degrees respectively. The plots show the dependence of the lift coefficient C_{LS} as defined by Shuford (based on the hull wetted surface area S) on the variation of the mean wetted length to beam at chines ratio. It is noted that the lift values predicted by CFD results are more close to the experimental ones than those predicted with the usual simplified methods, in all the analysed cases. Contextually it is also noted that the two formulations differ substantially among them, especially at small length to beam ratio (unfortunately in the range of values typical of actual planing boats). For $l_m/b < 2$ and trim angles greater than 2 degrees the error between the lift predicted with Savitsky and the experimental value is almost double of the error registered by the CFD predictions. A similarly good agreement is found with regards to the longitudinal position of the centre of pressure, as per figure 12. Finally, for what regards the resistance, as already noted in the previous section, the CFD results tend in general to underestimate the experimental values, and surprisingly correlate very well with Savitsky theory.

5. CONCLUSION AND FUTURE OUTLOOK

The paper presented in detail the set-up of a CFD model (in terms of mesh type, resolution, boundary conditions and turbulent flow models) able to reproduce the physical phenomena of the free surface flow in proximity a planing hull in a sufficiently accurate way. The CFD model was applied to the case of planing prismatic surfaces with a constant angle of 20 degrees, three different trim angles, typical of planing hull attitude, several relative speeds.

The validation of the CFD results against the reference experimental results is quite satisfactory. Except from few particular cases, the error between lift and drag and trim moment predicted by CFD code remain well inside the measuring error that affects the experimental results, with a marked tendency of the CFD prediction to underestimate the drag and lift forces. In general level of accuracy that can be expected from CFD predictions on model scale seems to be around 5% on (total) lift force and 10% on (total) drag force. Anyhow, it has been demonstrated that the error between the obtained CFD results and the experiments is much less than that registered by several semi-empirical formulations, such as that of Savitsky (1964) and Shuford (1956), still very widely used in the design of planing hull crafts.

For all the above mentioned findings, it can be concluded that the presented CFD model can be used with success for the hydrodynamic analysis and design of planing hulls and the same level of accuracy may be expected also in the case of "real" hulls with more complex shapes and appendages. Currently the authors are directing the investigation to the verification of the accuracy of CFD methods in the prediction of drag and running attitude of contemporary planing hulls shapes of various types and dimensions.

6. LIST OF SYMBOLS

Δ [kg]	Displacement at rest (weight)
R [kgf]	Total Resistance
F [kgf]	Friction Resistance
M [kgf·m]	Trim Moment (around transom bottom edge)
V [m/s]	Ship advance velocity
$C_{\Delta} = \Delta / wb^3$	Load Coefficient
$C_R = R / wb^3$	Resistance Coefficient
$C_v = V / \sqrt{gb}$	Froude number (based on breadth at chines) Shuford definition of C_L
$C_{ls} = \frac{\Delta}{0.5 \cdot \rho \cdot V^2 \cdot S}$	
τ [deg]	Trim Angle
β [deg]	Deadrise Angle
l_c [m]	Chine Wetted Length
l_k [m]	Keel Wetted Length
l_m [m] = $(l_c + l_k) / 2$	Mean Wetted Length
l_p [m] = $M / (\Delta \cdot \cos\tau + R \cdot \sin\tau)$	Ordinate of Press. centre
$b = 0.1016$ [m] $\equiv 4''$	Breadth at Chines
$S = l_m \cdot b^2$	Principal Wetted Area
$w = 1015.6$ [kg/m ³]	Specific weight of water (at test)

6. ACKNOWLEDGMENTS

The authors wish to thank the Hydrodynamic Research Office of Azimut group, in particular Mr. Bruckner and Mr. Delpini, for their support to this basic research project that set the foundation for the today achievement of good correlation in the more practical case of CFD calculation on real planing hull crafts.

REFERENCES

- CAPONNETTO M. (2001), 'Practical CFD Simulations for Planing Hulls', Proc. of Second International EuroConference on High Performance Marine Vehicles, HIPER'01, Hamburg, V. Bertram ed., pp.128-138.
- CHAMBLISS D.B., BOYD G.M. (1953), 'The Planing Characteristics of two V-shaped Prismatic Surfaces having angles of Deadrise of 20° and 40°', Langley Aeronautical Laboratory, NACA Technical Note 2876, Washington 1953.
- KAPRYAN W.J. AND WEINSTEIN I. (1952), 'The planing characteristics of a surface having a basic angle of dead rise of 20 degrees and horizontal chine flare', Langley Aeronautical Laboratory, NACA Technical Note 2804, 1952.
- KORVIN-KROUKOVSKY B.V, SAVITSKY D., LEHEMAN W.F. (1948), 'Wave Contours in the Wake of a 20° Deadrise Planing Surface', Davidson Lab., Report 337, Oct. 1948.
- PAYNE P.R. (1995), 'Contribution to planing Theory', Ocean Engineering, vol. 22, no.7, pp. 699-729.
- PEMBERTON R., TURNOCK S., WRIGHT A., BLAKE J. (2001), 'A Comparison of Computational Methods for Planing Crafts Hydrodynamics', Proc. of Second International EuroConference on High Performance Marine Vehicles, HIPER'01, V. Bertram ed., pp. 356-368.
- SHUFORD C.L. (1956), 'A Theoretical and Experimental Study of Planing Surfaces including effects of Cross Section and Plan Form', NACA Technical Note 3939, November 1956.
- SAVITSKY D. (1964), 'Hydrodynamic Design of Planing Hulls', Marine Technology, Volume 1, No.1, October 1964.

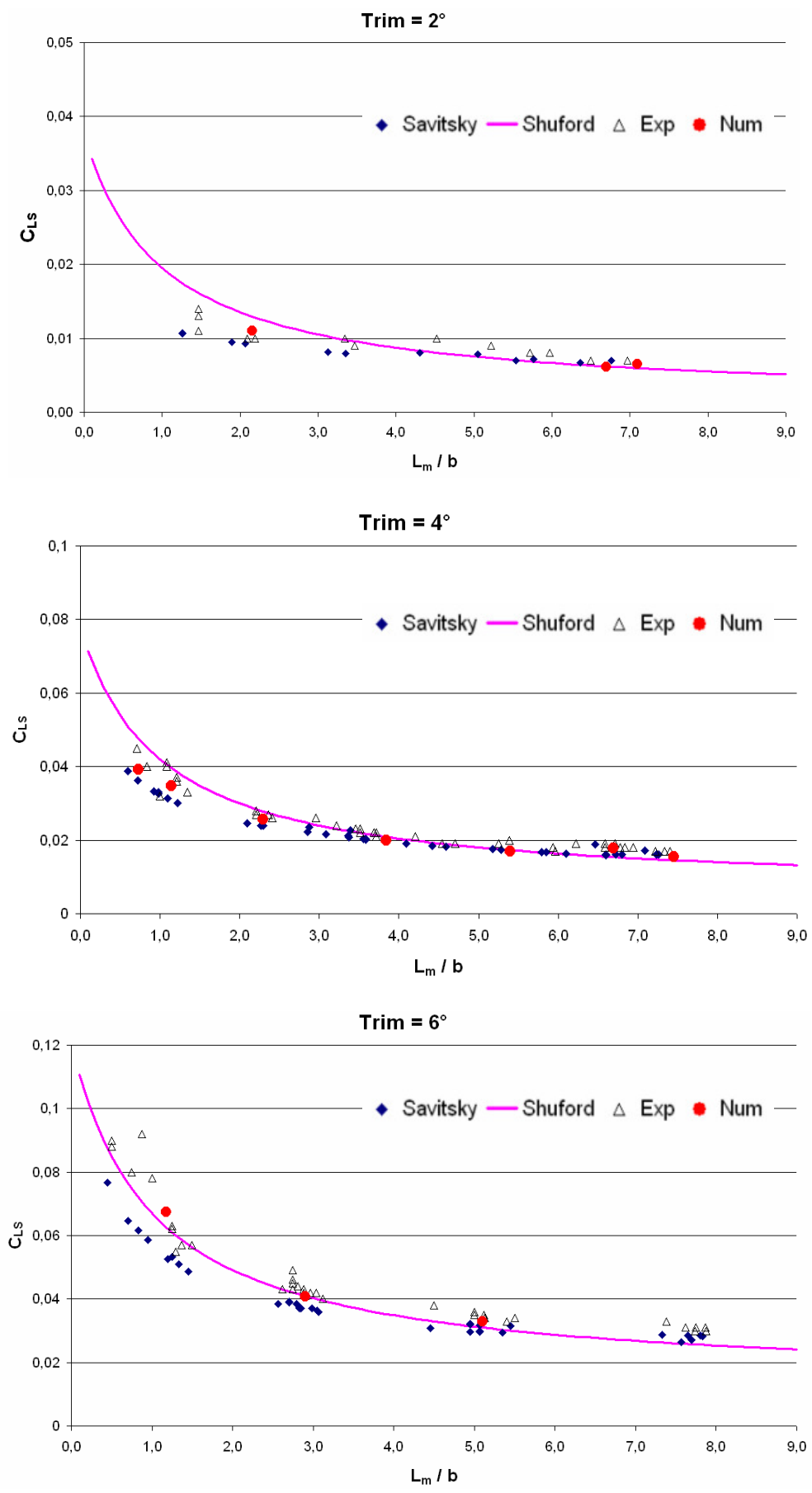


Figure 11
 Comparison of lift coefficient predicted by RANSE, with experiments, Savitsky and Shuford formulations

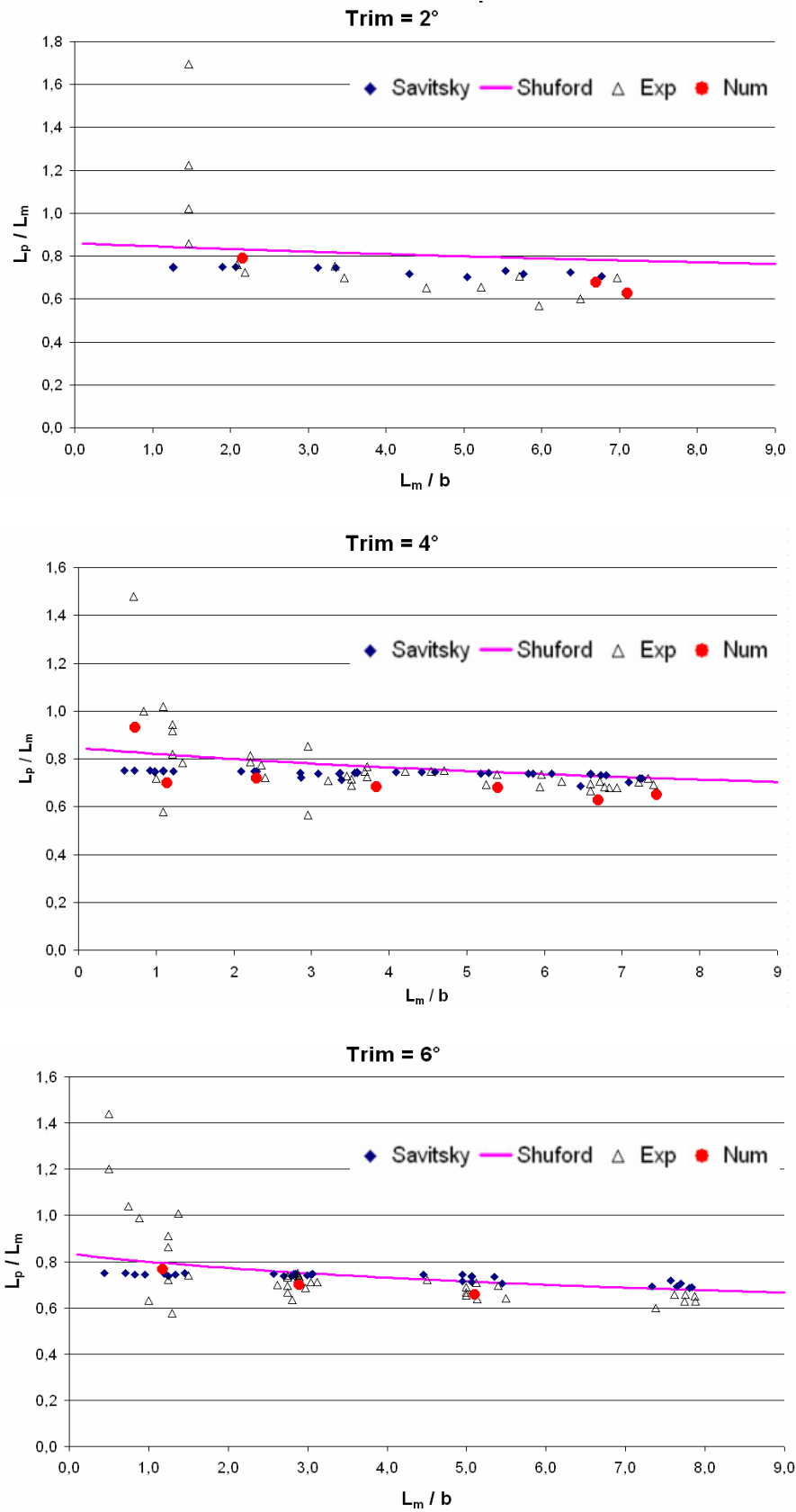


Figure 13
 Comparison of longitudinal centre of pressure predicted by RANSE,
 with the experimental one, and that calculated according Savitsky and Shuford formulations

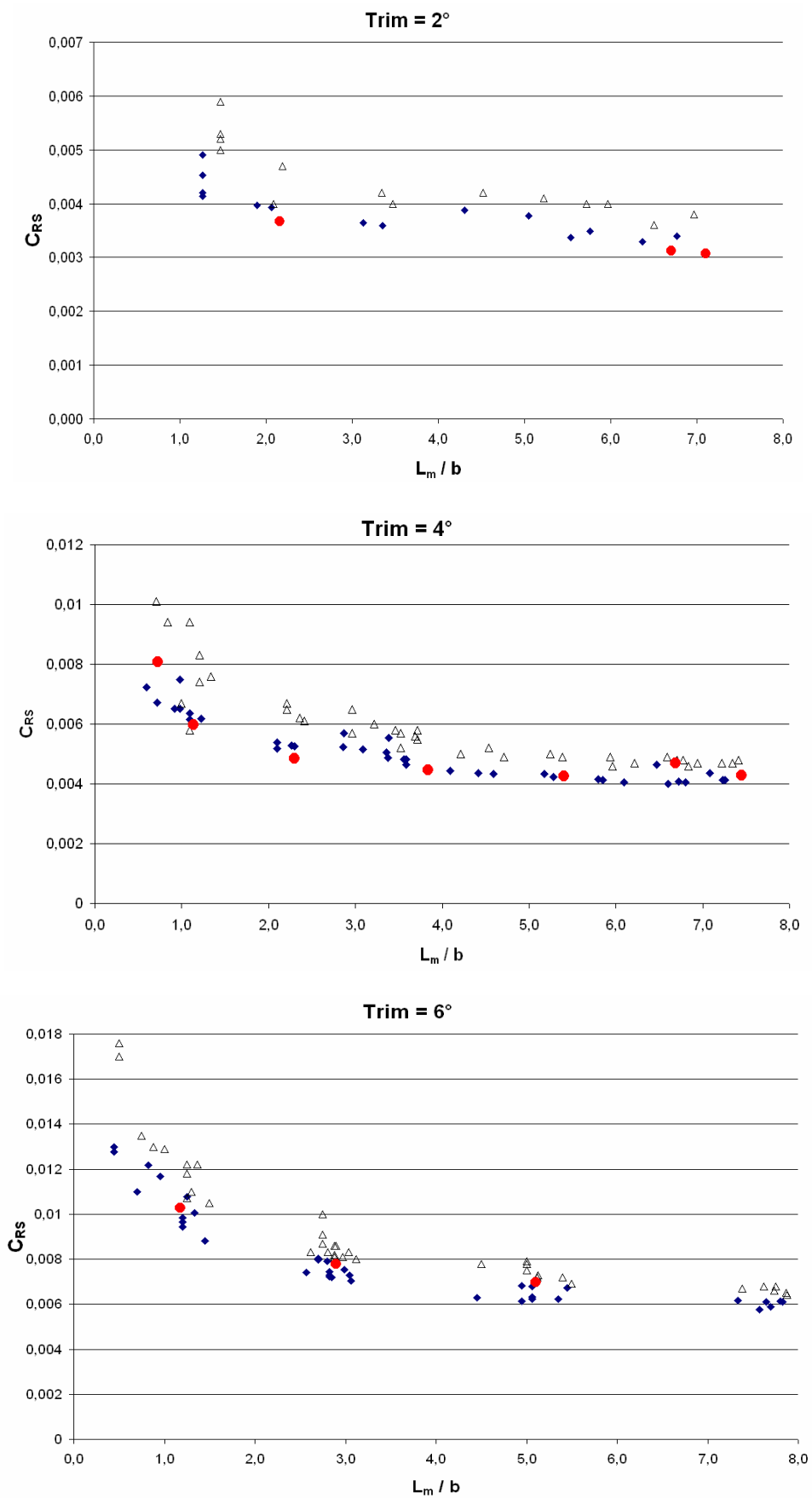


Figure 13
 Comparison of drag coefficient predicted by RANSE,
 with the experimental one and that calculated with Savitsky formulation